

See discussions, stats, and author profiles for this publication at: <https://www.researchgate.net/publication/231390206>

# Synthesis of Titanium-Containing Mesoporous Silicas as Catalysts for Cyclohexene Epoxidation

ARTICLE *in* INDUSTRIAL & ENGINEERING CHEMISTRY RESEARCH · SEPTEMBER 2009

Impact Factor: 2.59 · DOI: 10.1021/ie8018017

---

CITATIONS

18

---

READS

41

5 AUTHORS, INCLUDING:



**Mónica Crivello**

National University of Technology

27 PUBLICATIONS 441 CITATIONS

SEE PROFILE



**Eduardo Herrero**

National University of Technology

56 PUBLICATIONS 598 CITATIONS

SEE PROFILE



**Sandra G. Casuscelli**

National University of Technology

41 PUBLICATIONS 534 CITATIONS

SEE PROFILE

## KINETICS, CATALYSIS, AND REACTION ENGINEERING

## Synthesis of Titanium-Containing Mesoporous Silicas as Catalysts for Cyclohexene Epoxidation

Verónica R. Elías,<sup>†,‡</sup> Mónica E. Crivello,<sup>†</sup> Eduardo R. Herrero,<sup>†</sup> Sandra G. Casuscelli,<sup>†,‡</sup> and Griselda A. Eimer<sup>\*,†,‡</sup>

*Centro de Investigación y Tecnología Química (CITEQ), Facultad Regional Córdoba (FRC), Universidad Tecnológica Nacional (UTN), Maestro Lopez esq. Cruz Roja s/n, C. Universitaria, 5016, Córdoba, Argentina, and Consejo Nacional de Investigaciones Científicas y Técnicas (CONICET), Argentina*

Ti-containing mesoporous materials have been prepared by hydrothermal synthesis at 100 °C with two different Si/Ti ratios (20 and 60) in the synthesis mixture. A detailed study about the effect of synthesis time on the physicochemical properties of the materials has been carried out. The samples were characterized by XRD, DRUVvis, N<sub>2</sub> adsorption, and pyridine adsorption analyzed by FT-IR. The samples synthesized using the lower Si/Ti ratio presented the higher titanium incorporation and the higher acid character. The synthesis time appears as an important parameter that affects the textural, structural, chemical, and acid properties of the final solids. For the lower Si/Ti ratio, a longer synthesis time is needed to obtain a more ordered structure. However, in both cases, short synthesis times do not allow a proper incorporation of titanium into the silica framework, which is reached with synthesis times of about 3 days. The results of catalytic activity indicate that the solids studied here present an interesting potential as catalysts in the selective oxidation of cyclohexene using H<sub>2</sub>O<sub>2</sub>.

## 1. Introduction

Silica-based mesoporous materials with a tunable pore size (2–10 nm) and a large surface area (higher than 1000 m<sup>2</sup>/g) are of great interest because of their many potential applications in the pharmaceutical and fine chemical industries, in petroleum refining, and in adsorption and separation processes.<sup>1–5</sup> The catalytic properties of these materials rely on the presence of active sites in their frameworks. Consequently, many successful synthetic methods have been developed to prepare mesoporous silica with the incorporation of heteroelements into a silica framework in order to obtain high-performance catalysts. In the case of MCM-41, the introduction of titanium results in great interest in oxidation reactions especially of large molecules, which cannot diffuse in the pores of microporous materials.<sup>6–11</sup> Various authors have studied the catalytic performance of Ti-MCM-41 catalysts in the oxidation reactions of olefins. Sever et al.<sup>12</sup> reported a cyclohexene conversion near 23% with an epoxide selectivity about 11% over Ti-MCM-41 using a cyclohexene/H<sub>2</sub>O<sub>2</sub> molar ratio of 4. Hagen et al.<sup>13</sup> reported that the cyclohexene conversion was about 10% and the epoxide selectivity was lower than 5% on Ti-MCM-41 with H<sub>2</sub>O<sub>2</sub> as oxidant. Laha et al.<sup>14</sup> also reported low catalytic activity and low selectivity to cyclohexene oxide for Ti-MCM-41 in the presence of aqueous H<sub>2</sub>O<sub>2</sub>. Although other kind of materials such as Ti–silica mixed oxides have presented good results in the oxidation of olefins using organic hydroperoxides,<sup>15–17</sup> the use of hydrogen peroxide as oxidant results quite conveniently due to its easy handling, its high content of active oxygen, the absence of byproducts, and its relatively lower cost.<sup>18</sup>

It has recently been demonstrated<sup>10,19,20</sup> that the framework tetrahedral Ti(IV) species are the effective active sites for the

selective oxidation of olefins. In this respect, it has been shown that titanium can be successfully incorporated into the MCM-41 framework through a direct hydrothermal synthesis.<sup>21</sup> The porous structure and catalytic behavior of this system can be tailored to a certain extent by controlling the synthesis parameters such as titanium loading, surfactant/Si ratio, surfactant nature, and synthesis temperature. Although there are many reports concerning the synthesis and characterization of Ti-MCM-41 materials, the influence of some synthesis parameters, such as synthesis time, on their structural and catalytic properties has not been completely elucidated. Since the rates of polymerization of the silicon and titanium species are different, the synthesis time must be also an important parameter that can affect not only the textural and chemical properties of the final solid but also the present metallic species.

The aim of the present work was to study the influence of the synthesis time in two series of MCM-41 materials, prepared by hydrothermal synthesis with different Si/Ti molar ratios in the synthesis gel, over their physicochemical properties. Such synthesis variables were manipulated in order to maximize the presence of catalytically active sites in the material, analyzing specifically the local environment of Ti(IV) centers within the silica matrix. The surface acidity associated with the presence of these active sites was monitored by using in situ Fourier transform infrared spectroscopy (FT-IR) of pyridine adsorption. The catalytic properties of these materials were tested for the cyclohexene oxidation reaction with H<sub>2</sub>O<sub>2</sub>.

## 2. Experimental Section

The titanium-containing mesoporous materials were prepared by hydrothermal synthesis using dodecyltrimethylammonium bromide (DTMABr) as a template. Tetraethoxysilane (TEOS) and titanium isopropoxide (TIP) were used as the Si and Ti sources, respectively. The catalysts were synthesized from gel

\* To whom correspondence should be addressed. E-mail: geimer@scdt.frc.utn.edu.ar.

<sup>†</sup> UTN.

<sup>‡</sup> CONICET.

of molar compositions Si/Ti = 20 and 60, OH/Si = 0.30, surfactant/Si = 0.4, and water/Si = 60. In a typical synthesis, TEOS (Fluka,  $\approx 98\%$ ) and TIP (Fluka,  $\approx 98\%$ ) were vigorously mixed for 30 min. Then, a 25 wt % solution of DTMABr (Fluka,  $\approx 98\%$ ) in ethanol and 70% of the tetraethylammonium hydroxide 20 wt % aqueous solution (TEAOH) (Fluka) were added dropwise under stirring, which was continued for 3 h. Finally, both the remaining TEAOH and the water were added dropwise to the milky solution, which was then heated at 353 K for 30 min to remove both the ethanol used in the solution and the additional one produced in the TEOS hydrolysis. The pH of the resultant gel was 11.5. This gel was transferred into Teflon-lined stainless-steel autoclave and kept in an oven at 100 °C for 0–7 days under autogenous pressure. The solid was then filtered off, washed with distilled water, and dried at 60 °C overnight. To remove the template, the samples were heated (heating rate of 2 °C/min) under N<sub>2</sub> flow up to 500 °C maintaining this temperature for 6 h and subsequently calcined at 500 °C under air flow for 6 h.

The titanium content in the final solid products was determined by inductively coupled plasma atomic emission spectroscopy (ICP-AES) in a VG Elemental Plasma Quad 3 mass spectrometer. X-ray powder diffraction (XRD) patterns were collected in air on a Philips PW 3830 diffractometer at room temperature using Cu K $\alpha$  radiation of wavelength 0.154 18 nm. Diffraction data were recorded between 1 and 40° at an interval of 0.01° and a scanning speed of 2°/min was used. The structural ordering degree of each sample was calculated against an *internal standard sample* which was arbitrarily considered as a *reference*. Such a sample showed the highest intensity for the (100) diffraction peak, assuming a 100% structural ordering for this sample. Diffuse reflectance UV–visible (DRUVvis) spectra were recorded using a Perkin-Elmer Lambda 35 spectrometer in the wavelength range 200–400 nm. The specific surface area of all the samples was determined using a Pulse Chemisorb equipment. The samples were previously dried at 400 °C under N<sub>2</sub> flow for 2 h. The N<sub>2</sub> adsorption–desorption isotherms were obtained at 77 K using a Micromeritics ASAP 2010 equipment. The surface area was calculated by the BET method in the  $P/P_0$  range 0.05–0.1 in order to ensure the BET equation linearity. Density function theory method (DFT) was applied to evaluate the pore size distribution since this method, based on a molecular statistical approach, is applied over the complete range of the isotherm.<sup>22</sup>

The acid properties of the samples were evaluated by FT-IR spectral measurements of pyridine adsorption performed on a JASCO 5300 spectrometer, through the following procedure. A self-supporting wafer for each sample ( $\sim 20$  mg/cm<sup>2</sup>) was prepared, placed in a thermostated cell with CaF<sub>2</sub> windows connected to a vacuum line, and evacuated for 8 h at 400 °C. The background spectrum was recorded first after cooling the sample to room temperature. Afterward, the solid wafer was exposed to pyridine vapors at room temperature and allowed to saturate for 20 min. The IR spectrum for each sample was obtained after pyridine desorption by evacuation for 1 h at 200, 300, and 400 °C. The difference spectrum was obtained finally by subtracting the background spectrum recorded previously.

The cyclohexene oxidation reactions with H<sub>2</sub>O<sub>2</sub> were carried out at 70 °C under stirring in 2 mL glass vials immersed in a thermostatted bath. Typically, the reaction mixture consisted of 9.00 mg of catalyst, 91.90 mg of cyclohexene (Baker,  $\approx 98\%$ ), 26.60 mg of oxidant (hydrogen peroxide 35% w/w, Riedel-de Haen), and 678.30 mg of solvent (acetonitrile, Cicarelli). In all cases the oxidant to substrate molar ratio was 1:4 in order to

**Table 1. Synthesis Parameters and Physical Properties of the Synthesized Samples**

sample	Si/Ti <sup>a</sup>	synth time (days)	$a_0$ (Å)	surf. area <sup>b</sup> (m <sup>2</sup> /g)
TiM-20-0	20	0	34.6	895
TiM-20-1	20	1	37.3	871
TiM-20-3	20	3	37.0	895
TiM-20-5	20	5	36.9	1145
TiM-20-7	20	7	37.2	886
TiM-60-0	60	0	35.4	956
TiM-60-1	60	1	36.4	1235
TiM-60-3	60	3	36.1	1206
TiM-60-5	60	5	33.3	1073
TiM-60-7	60	7	32.5	1119

<sup>a</sup> In synthesis gel. <sup>b</sup> BET specific surface area.

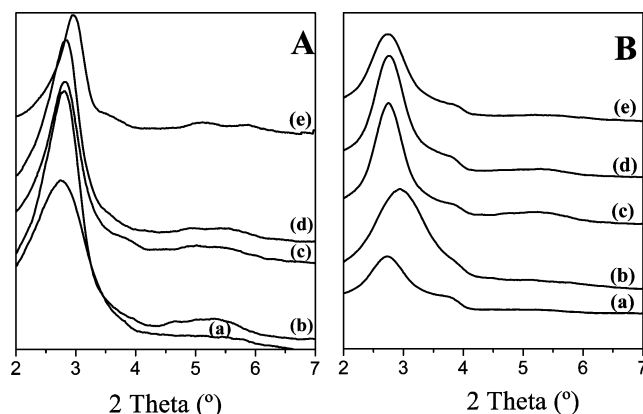


**Figure 1.** XRD patterns of the samples synthesized with Si/Ti molar ratios in the synthesis mixture: (A) 60 and (B) 20. Synthesis times: (a) 0, (b) 1, (c) 3, (d) 5, and (e) 7 days.

minimize the possible Ti leaching.<sup>23</sup> The reaction products were analyzed by gas chromatography (Hewlett-Packard 5890 Series II) using a capillary column (cross-linked methyl silicone gum, 30 m long) and flame ionization detector. Additionally, the GC–MS (Shimadzu, QP 5050 A) analyses were performed in order to identify the products. The total conversion of H<sub>2</sub>O<sub>2</sub> was measured by iodometric titration. The cyclohexene conversion was defined as cyclohexene conversion  $\times$  100/theoretically possible conversion (% of maximum).

### 3. Results and Discussion

Table 1 summarizes the physical properties of the samples prepared in this study with two different Si/Ti molar ratios (20 and 60) in the synthesis mixture and synthesis times of 0–7 days. The XRD patterns of these samples, with a 0.02° precision at the peak maximum, are shown in Figure 1. Although all the samples exhibit an intense low-angle reflection at approximately 2.5–3.0°, characteristic of mesoporous materials, the mesostructures prepared with the lowest Ti content exhibit two other weak peaks ascribed to (110) and (200) reflections characteristic of a MCM-41 structure. As it is known, the number of well-defined peaks and their relative intensities represent the relative structural ordering of an MCM-41 structure. Thus, the broadening and intensity decreasing of X-ray reflections with the Ti content in the synthesis mixture (Si/Ti molar ratio = 20) can be attributed to a lowering of the lattice order, which can also be correlated with a decrease in the surface area observed. The bond length of Ti–O different from that of tetrahedral Si–O should distort the geometry, leading to some structure deformation. Moreover, the presence of some Ti–O–Ti clustering could be contributing to the deterioration of the mesoporous structure as the Si/metal ratio decreases. Nevertheless, it is important to

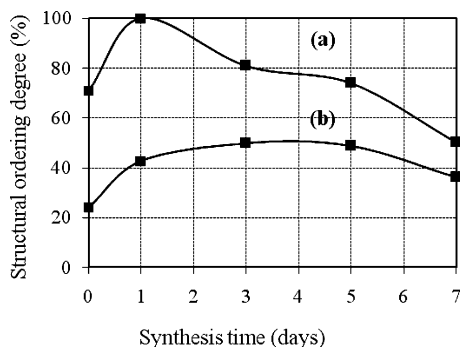


**Figure 2.** Effect of synthesis time on the degree of structural ordering of the samples synthesized with Si/Ti molar ratio in the synthesis mixture: (a) 60 and (b) 20.

remark that while the material synthesized with the higher Ti loading shows a modest degree of order, the same allowed a maximum incorporation of Ti of 2.5 wt % without collapsing the structure. In addition, the main XRD peak slightly shifts toward a lower diffraction angle and a slight increase in the parameter  $a_0$  is detected as the content of Ti is increased (Table 1). Taking into account that the Ti–O–Si bond length is longer than the Si–O–Si one, this feature may be consistent with the probable incorporation of Ti into the mesoporous framework.

Even though the mesostructure was formed before the hydrothermal treatment, the structural ordering was increased when the samples were hydrothermally treated. However, a different effect of hydrothermal synthesis time on such ordering was observed for the different Ti contents in the material. This effect was analyzed for the two different initial Si/Ti ratios (20 and 60), evaluating the structural ordering degree of each sample in comparison to a sample arbitrarily taken as reference with 100% ordering (Si/Ti = 60 and hydrothermal synthesis of 1 day).<sup>24</sup> Figure 2 shows that a longer synthesis time is needed to obtain a more ordered structure when the Si/Ti ratio in the synthesis mixture is decreased. Although the maximum structural ordering is quickly reached for the higher Si/Ti ratio, a synthesis beyond 1 day appears to induce some disorder in the structure. These results are in agreement with previous reports by Cedeño et al.<sup>25</sup> In contrast, in the case of the lower Si/Ti ratio, the maximum ordering obtained is practically not affected by an increase in the synthesis time. On the other hand, while all the samples exhibit surface areas above 1000 m<sup>2</sup>/g, these areas reach a maximum value for the optimum synthesis time that leads to the more ordered structure in each case.

DRUVvis spectroscopy is a very sensitive method for characterization of the coordination environment of titanium in zeolite framework.<sup>26,27</sup> DRUVvis spectra of all the samples synthesized are shown in Figure 3. An intense DRUVvis band at 210 nm in all the samples indicates that most of the Ti species are isolated and in tetrahedral coordination inside the framework.<sup>21,28–30</sup> Another band at 260 nm, more significant for the samples with higher Ti content, can be attributed to the presence of partially polymerized Ti–O–Ti species probably originated by the rate of polymerization of TIP higher than the one of TEOS.<sup>28,29,31</sup> Such Ti–O–Ti clustering could be contributing, although slightly, to the lower structural ordering and surface area observed for these samples.<sup>19,21</sup> Furthermore, the presence of higher coordinated Ti species probably due to the insertion of water molecules upon hydration should be also considered.<sup>32</sup> On the other hand, the lack of an absorption band at about 300–330 nm allowed us to confirm the absence of a segregated anatase phase in the samples.<sup>21,28–30</sup> It should be noted that the maximum incorporation of Ti in the materials was about

2.5% and 1.1% for the Si/Ti ratios 20 and 60, respectively, and both catalysts present most of the Ti occupying isolated positions in the framework. Moreover, in contrast with other results,<sup>28</sup> the intensity of the 210 nm band is substantially increased and the position of the maximum does not shift toward higher wavelengths with increasing Ti content. Such a behavior suggests that the tetrahedral component of Ti(IV) is prevalent even in the sample synthesized with high Ti content.

As can be observed in Figure 3, the magnitude of the absorption depends on the synthesis time. For both Si/Ti ratios in the initial mixture, titanium is not well incorporated into the silica framework at short synthesis times. Meanwhile, a synthesis time of about 3 days seems to be necessary to allow a proper incorporation of titanium into the silica framework. It is noticeable that the sample synthesized with lower Si/Ti ratio and synthesis time of 3 days exhibits the highest Ti incorporation, which seems to be almost unaffected by a longer synthesis time (7 days). In contrast, in the case of the samples with lower Ti content (Si/Ti ratio = 60), a long synthesis time (7 days) shows a light decrease of the Ti incorporation, which would be probably consistent with the decrease of structural ordering and surface area.

The chemisorption of pyridine followed by IR studies is usually a useful probe to detect the presence and nature of acid sites on a catalyst surface.<sup>20</sup> The FT-IR spectra of adsorbed pyridine on the samples synthesized (Figure 4) show that the same exhibit Lewis acidity, evidenced by the presence of the bands at 1610 and 1449 cm<sup>-1</sup>.<sup>25,30,33,34</sup> However, it is necessary to clarify here that this last band at 1449 cm<sup>-1</sup> appears overlapped with the one corresponding to hydrogen bonded pyridine.<sup>20</sup> It is known that pyridine can form hydrogen bonds with the silanol groups present in the structure, showing typical bands at 1447 and 1599 cm<sup>-1</sup>.<sup>30,33,34</sup> In addition, these samples also present some Brønsted acidity, evidenced by weak bands at 1540 and 1636 cm<sup>-1</sup>.<sup>33,35</sup> Some changes in the acidity with the synthesis time can be observed. It is noteworthy that, for both Si/metal ratios, the acidity reaches the maximum when the synthesis time is about 3 days and decreases with longer synthesis times (7 days). As it is known, the strength of Lewis and Brønsted acid sites can be obtained from pyridine thermodesorption. Thus, as the heating temperature reached 300 °C under vacuum (Figure 4C,D), the intensities of all the bands decreased. In addition, whereas the bands assigned to Lewis sites undergo a further reduction after desorption at 400 °C, those corresponding to Brønsted sites tend to disappear (Figure 4E,F). Such a feature indicates that whereas the Lewis sites are strong enough to retain the pyridine molecules until 400 °C, the Brønsted sites present a rather weak character. The above results are according to the changes observed in the DRUVvis spectra with the synthesis time suggesting, besides, that the incorporation of titanium into the silica framework generates acid sites.<sup>20</sup> Therefore, it seems that there is an optimum synthesis time, which leads to a greater amount of titanium incorporated and a high concentration of acid sites.

On the other hand, Figure 5 shows the adsorption/desorption isotherms of the samples prepared with two different Si/Ti ratios (20 and 60) and 3 days of hydrothermal synthesis. Both samples exhibit type IV isotherms typical of mesoporous structures with a sharp inflection at relative pressure ( $P/P_0$ ) of 0.1–0.25 characteristic of capillary condensation inside the conventional mesopores present in the MCM-41 structure. Such an inflection is evidence of a narrowly defined diameter range for mesoporous channels of these materials, which is also reflected in Figure 6. The pore diameter for both samples is around 27 Å. For the



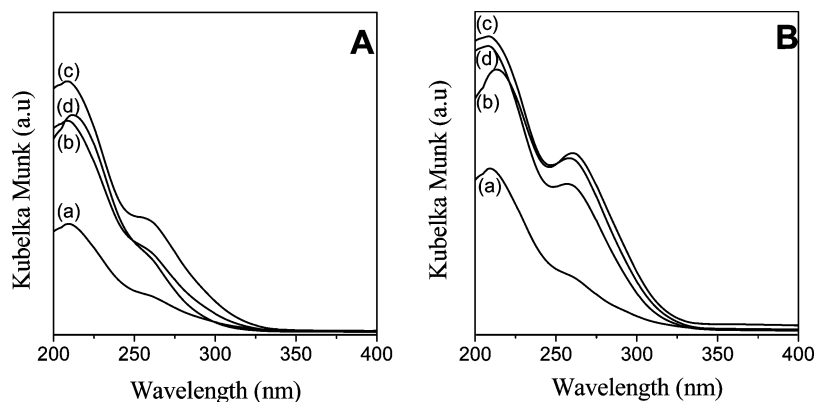


**Figure 3.** DRUVvis spectra of the samples synthesized with Si/Ti molar ratios in the synthesis mixture: (A) 60 and (B) 20. Synthesis times: (a) 0, (b) 1, (c) 3, and (d) 7 days.

**Scheme 1. Products of Cyclohexene Oxidation with Hydrogen Peroxide Catalyzed by Ti-MCM-41: Cyclohexene Oxide (I), 1,2-Cyclohexanediol (II), 2-Cyclohexen-1-one (III), and 2-Cyclohexen-1-ol (IV)**

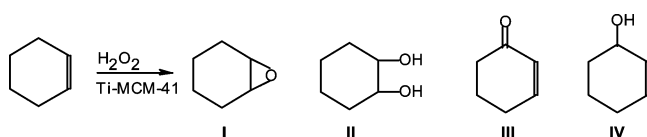


**Table 2. Catalytic Activity in the Cyclohexene Oxidation Reaction<sup>a</sup>**

sample	cyclohexene conversion (% of max)	H <sub>2</sub> O <sub>2</sub> selectivity (%) <sup>b</sup>	selectivity (% mol)			
			I	II	III	IV
TiM-20-3	66.4	76	37.5	26.3	17.5	18.7
TiM-60-3	57	77	40	12.5	25	22.5

<sup>a</sup> Reaction conditions: cyclohexene/H<sub>2</sub>O<sub>2</sub> (mol/mol) = 4; catalyst = 9.79% of the substrate; temperature = 70 °C; reaction time = 5 h.

<sup>b</sup> H<sub>2</sub>O<sub>2</sub> selectivity defined as the moles of products formed/mol of H<sub>2</sub>O<sub>2</sub> reacted.

**Table 3. Catalytic Performance of Recovered TiM-20-3 in Cyclohexene Oxidation with H<sub>2</sub>O<sub>2</sub>**

catalytic cycle	cyclohexene conversion (% of max)	selectivity (% mol)			
		I	II	III	IV
1	66.4	37.5	26.3	17.5	18.7
2	66.1	37.3	26.8	18	17.9
3	66.5	36.9	26.7	17.4	19
4	66.0	37.6	26.5	17.5	18.4

sample prepared with the higher Si/Ti ratio, a very small hysteresis loop is additionally observed in the isotherm. Meanwhile, the isotherm of the sample prepared with the higher Ti content shows the presence of a pronounced hysteresis loop which could be associated with a capillary condensation in secondary mesopores.<sup>21,36–38</sup> The titanium seems to be responsible for the presence of the hysteresis showing a specific role in the development of this secondary porosity, which might have great relevance for catalysis as it would probably enhance the diffusion of reagents through the particles.

The oxidation of cyclohexene using hydrogen peroxide is frequently used as a test reaction for the catalytic evaluation of different titanium-modified materials. It is known that the Ti species in framework positions are the active sites for carrying out selective catalytic oxidations of hydrocarbons using peroxides as oxidants. Moreover, TiO<sub>2</sub> crystals with an anatase structure in the titanasilicates were proved to lower the catalytic performance by enhancing the decomposition of H<sub>2</sub>O<sub>2</sub> into water and oxygen. Therefore, it becomes crucial to find the synthesis

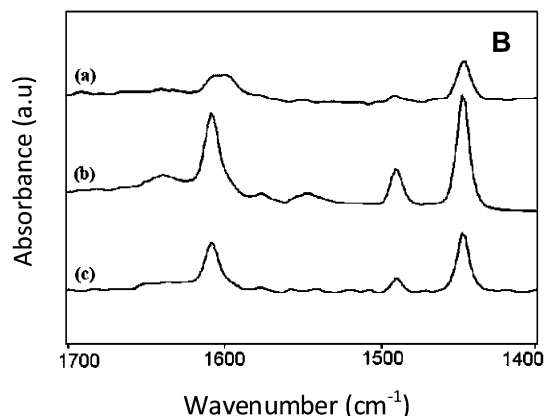
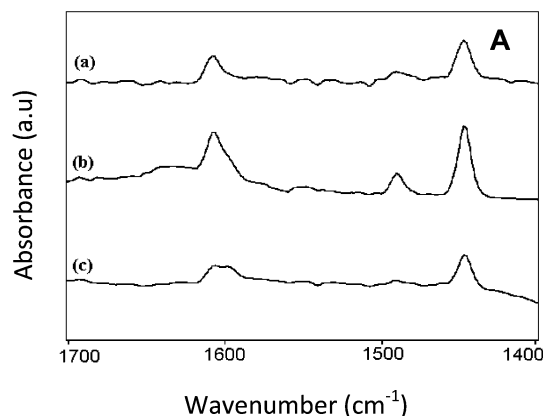
parameters, such as the optimum synthesis time, in order to maximize the presence of Ti species incorporated into the framework.<sup>39</sup>

Scheme 1 illustrates some of the typical products of cyclohexene oxidation. The cyclohexene oxide (I), generated by the heterolytic epoxidation of the cyclohexene double bond, and the 1,2-cyclohexanediol (II) side product, formed by hydrolysis of the epoxide ring, generally reflect a concerted process. In contrast, the allylic oxidation side products, 2-cyclohexen-1-one (III) and 2-cyclohexen-1-ol (IV), are often ascribed to a homolytic radical pathway.<sup>12</sup>

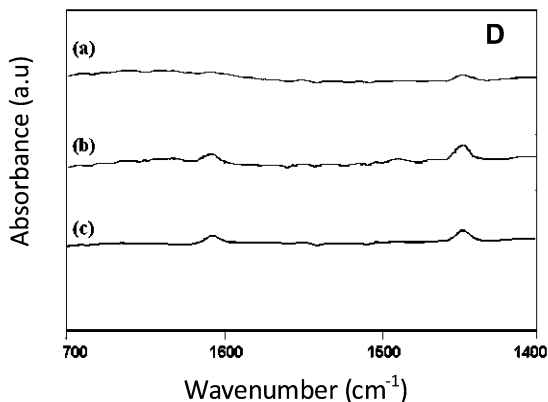
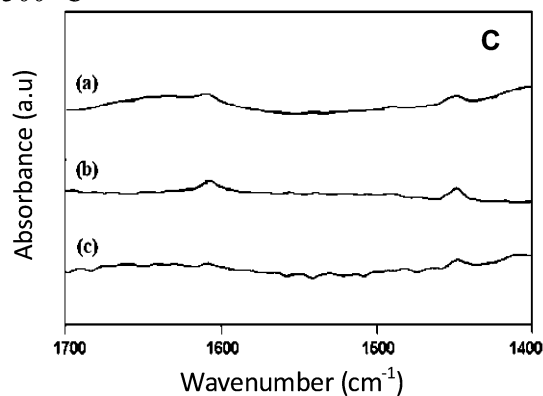
The results of the catalytic activity measurements obtained with the samples prepared with 3 days synthesis time and Si/Ti ratio of 20 and 60 are shown in Table 2. It should be noted that such samples were selected taking into account both an adequate structural quality and a maximum of framework Ti species. Both samples show good catalytic activity in the oxidation reaction studied. The cyclohexene conversion values increase when the Si/Ti ratio decreases, which is according to the increase for Ti species in framework positions evidenced by the DRUVvis analysis. Therefore, such a feature corroborates that the titanium incorporated into the framework is actually the active species for the selective oxidation of olefins using H<sub>2</sub>O<sub>2</sub>. It is noteworthy that the epoxide is the main reaction product for both samples; however, its selectivity decreases whereas the selectivity toward glycol increases for the sample with lower Si/Ti ratio. It is known that the epoxides can easily react with water to form glycol further catalyzed by acid sites. Thus, the acidity of the material may markedly influence the final product composition. Therefore the observed results can be attributed to an epoxide ring-opening reaction with water that leads to the formation of 1,2-cyclohexanediol as side product. This product would be favored by the increasing acidity evidenced by the FT-IR spectrum of the TiM-20-3 sample (Figure 4). On the other hand, the products arising from the allylic oxidation side reaction are observed to a small extent to be unfavored by the Ti loading growing. It is very important to note here that, in contrast to other authors who report cyclohexene conversions on Ti-MCM-41 of about 10–20% and epoxide selectivities of about 5–10%,<sup>12,13,40</sup> our catalysts exhibit a maximum conversion of 66% with a high selectivity to epoxide (about of 40%) under similar reaction conditions. Otherwise, an epoxide selectivity of about 50% has been reported for the cyclohexene oxidation on TiO<sub>2</sub>–SiO<sub>2</sub> mixed oxides when 1,2-dimethoxyethane is used as solvent in place of acetonitrile.<sup>16</sup>

As it was just explained, the isolated tetrahedral Ti(IV) species in the framework are the active sites responsible for the direct

200 °C



300 °C



400 °C

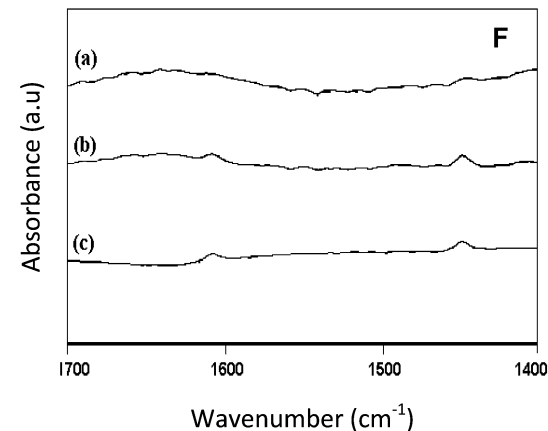
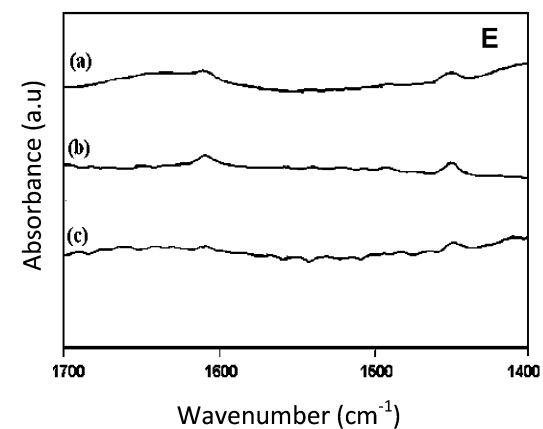


**Figure 4.** FT-IR spectra of pyridine adsorbed on the samples synthesized. Desorption at temperature 200 °C: (A) Si/Ti:60, (B) Si/Ti:20. Desorption temperature at 300 °C: (C) Si/Ti:60, (D) Si/Ti:20. Desorption temperature at 400 °C: (E) Si/Ti:60, (F) Si/Ti:20. Synthesis time: (a) 1, (b) 3, and (c) 7 days.

epoxidation of olefins using peroxides as oxidants and the decomposition of  $\text{H}_2\text{O}_2$  into water and oxygen, favored by the presence of anatase, is the main side reaction for this peroxide. As can be seen in Table 2, our catalysts synthesized with both Si/Ti ratios presented a high peroxide selectivity of around 75%. This feature reveals that a considerable amount of  $\text{H}_2\text{O}_2$  has been used for the oxidation reaction, which supports the case for well-dispersed Ti present on our materials. Although there are various reports about the catalytic performance of Ti-MCM-41 materials in the oxidation reaction of cyclohexene with  $\text{H}_2\text{O}_2$ ,<sup>12–14,42</sup> the  $\text{H}_2\text{O}_2$  selectivity values are often not reported. In this respect, Server et al.<sup>12</sup> reported a  $\text{H}_2\text{O}_2$  selectivity of 67.7% which was increased up to 74.5% when the Ti-MCM-41 catalyst underwent a silylation treatment. It is important to

note here that our selectivity result of about 75% was obtained for a Ti-MCM-41 catalyst without any postsynthesis treatment.

In order to evaluate the propensity to be recovered and recycled, the catalysts underwent four 5-h catalytic cycles overall. The calcination step before each recycle would lead to the elimination of adsorbed byproduct that hinders the coordination of the reagents to the active centers. Table 3 shows the cyclohexene conversion and selectivity to products for each run on TiM-20-3, which is given as an example. As can be seen, the catalytic activity remained almost constant after the fourth run and the product selectivity did not change remarkably on passing from the first to the fourth catalytic run. These results suggest that there is not a valuable modification of the catalytic active sites during the recycling steps. In fact, as demonstrated

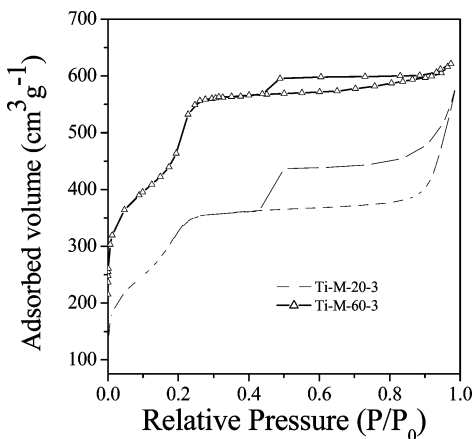


**Figure 5.** Nitrogen adsorption-desorption isotherms of the TiM-20-3 and TiM-60-3 samples.

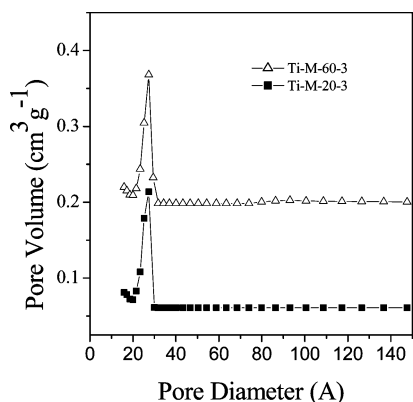


**Figure 6.** DFT pore size distribution of the TiM-20-3 and TiM-60-3 samples.

by ICP and DRUVvis, almost no Ti leaches out and no Ti species leave their original location even after four catalytic cycles.<sup>23</sup> Moreover, no structural changes occurred in the catalyst throughout the cycles since its XRD pattern was not modified. Therefore, in contrast with other authors who reported Ti leaching during the liquid phase reaction,<sup>41–44</sup> the catalysts prepared via our synthesis method exhibited good stability under the employed conditions, being regenerated repeatedly without suffering loss in activity.

#### 4. Conclusions

All the above results indicate that the synthesis time has a definitive influence in the textural, structural, and chemical properties of titanium-modified mesoporous silica. Moreover, such effects are different depending on the amount of titanium present in the synthesis mixture. Although a lower degree of structural ordering was observed in the samples with the lower Si/Ti ratio, a higher amount of titanium could be incorporated into the framework. In the case of the lower Si/Ti ratio, the more ordered structures are more slowly reached but long synthesis times (about 7 days) appear not to influence the ordering degree. For both Si/Ti ratios analyzed, short synthesis times do not allow an adequate incorporation of titanium into the silica framework. Meanwhile, this is successfully achieved at a synthesis time of about 3 days, which also leads to a higher concentration of acid sites. The titanium-containing materials synthesized here showed very good activity for the oxidation of cyclohexene using  $\text{H}_2\text{O}_2$ . The main oxidation product was the cyclohexene epoxide. The glycol appears as a byproduct,

which is favored by the increasing acidity of the material. The products of allylic oxidation are observed to a small extent to be unfavored by the Ti loading growth. Finally, the catalysts could be recycled after regeneration without suffering activity loss.

#### Acknowledgment

The authors wish to thank J. D. Fernández for assistance with surface area and FT-IR measurements. The authors also thank H. Thomas and N. Firpo (CINDECA, La Plata, Argentina) for help in recording DRUVvis data.

#### Literature Cited

- (1) Kresge, C.; Leonowicz, M.; Roth, W.; Vartuli, J.; Beck, J. Ordered Mesoporous Molecular Sieves Synthesized by a Liquid Crystal Template Mechanism. *Nature* **1992**, 359, 710.
- (2) Vartuli, J.; Schmidt, K.; Kresge, C.; Roth, W.; Leonowicz, M.; McCullen, S.; Hellring, S.; Beck, J.; Schlenker, J.; Olson, D.; Sheppard, E. Effect of Surfactant/Silica Molar Ratios on the Formation of Mesoporous Molecular Sieves: Inorganic Mimicry of Surfactant Liquid-Crystal Phases and Mechanistic Implication. *Chem. Mater.* **1994**, 6, 2317.
- (3) Corma, A. From Microporous to Mesoporous Molecular Sieve Materials and Their Use in Catalysis. *Chem. Rev.* **1997**, 97, 2373.
- (4) Ghanbari-Siahkhalil, A.; Philippou, A.; Dwyer, J.; Anderson, M. The Acidity and Catalytic Activity of Heteropoly Acid on MCM-41 Investigated by MAS NMR, FTIR and Catalytic Test. *Appl. Catal., A* **2000**, 192, 57.
- (5) Trong On, D.; Desplandier-Giscard, D.; Danumah, C.; Kaliaguine, S. Perspectives in Catalytic Applications of Mesoporous Materials. *Appl. Catal., A* **2001**, 222, 299.
- (6) Berlino, C.; Guidotti, M.; Moretti, G.; Psaro, R.; Ravasio, N. Catalytic Epoxidation of Unsaturated Alcohol on Ti-MCM-41. *Catal. Today* **2000**, 60, 219.
- (7) Berlino, C.; Ferraris, G.; Guidotti, M.; Moretti, G.; Psaro, R.; Ravasio, N. A. Comparison between [Ti]-MCM-41 and Amorphous Mesoporous Silica-Titania as Catalyst for the Epoxidation of Bulky Unsaturated Alcohol. *Microporous Mesoporous Mater.* **2001**, 44–45, 595.
- (8) Gallo, J.; Paulino, I.; Schuchardt, U. Cyclooctene Epoxidation using Nb-MCM-41 and Ti-MCM41 Synthesized at Room Temperature. *Appl. Catal., A* **2004**, 266, 223.
- (9) Guidotti, M.; Ravasio, N.; Psaro, R.; Ferraris, G.; Moretti, G. Epoxidation on Titanium-containing Silicates: do Structural Features Really Affect the Catalytic Performance. *J. Catal.* **2003**, 214, 242.
- (10) Casuscelli, S.; Eimer, G.; Canepa, A.; Heredia, A.; Poncio, C.; Crivello, M.; Perez, C.; Aguilar, A.; Herrero, E. Ti-MCM-41 as Catalyst for  $\alpha$ -Pinene Oxidation. Study of the Effect of Ti Content and  $\text{H}_2\text{O}_2$  Addition on Activity and Selectivity. *Catal. Today* **2008**, 133–135, 678.
- (11) Corma, A.; Navarro, M.; Perez-Pariente, J. Synthesis of an Ultralarge Pore Titanium Silicate Isomorphous to MCM-41 and its Applications as a Catalyst for Selective Oxidation of Hydrocarbons. *J. Chem. Soc., Chem. Commun.* **1994**, 147.
- (12) Sever, R.; Alcalá, R.; Dumesic, J.; Root, T. Vapor-Phase Silylation of MCM-41 and Ti-MCM-41. *Microporous Mesoporous Mater.* **2003**, 66, 53.
- (13) Hagen, A.; Schueler, K.; Roessner, F. The performance of Ti-MCM-41 in Aqueous Media and After Mechanical Treatment Studied by in situ XANES, UV/Vis and Test Reactions. *Microporous Mesoporous Mater.* **2002**, 51, 23.
- (14) Laha, S.; Kumar, R. Promoter-Induced Synthesis of MCM-41 type Mesoporous Materials Including Ti- and V-MCM-41 and their Catalytic Properties in Oxidation Reactions. *Microporous Mesoporous Mater.* **2002**, 53, 163.
- (15) Dutoit, D.; Schneider, M.; Baiker, A. Titania-Silica Mixed Oxides I. Influence of Sol-Gel and Drying Conditions on Structural Properties. *J. Catal.* **1995**, 153, 165.
- (16) Kochkar, H.; Figueras, F. Synthesis of Hydrophobic  $\text{TiO}_2$ - $\text{SiO}_2$  Mixed Oxides for the Epoxidation of Cyclohexene. *J. Catal.* **1997**, 171, 420.
- (17) Hutter, R.; Mallat, T.; Baiker, A. Titania-Silica Mixed Oxides II. Catalytic Behaviour in Olefin Epoxidation. *J. Catal.* **1995**, 153, 177.
- (18) Sanderson, W. Cleaner Industrial Processes using Hydrogen Peroxide. *Pure Appl. Chem.* **2000**, 72, 1289.
- (19) Eimer, G.; Casuscelli, S.; Ghione, G.; Crivello, M.; Herrero, E. Synthesis, Characterization and Selective Oxidation Properties of Ti-containing Mesoporous Catalyst. *Appl. Catal., A* **2006**, 298, 232.

- (20) Eimer, G.; Casuscelli, S.; Chanquia, C.; Elías, V.; Crivello, M.; Herrero, E. The Influence of Ti-loading on the Acid Behavior and on the Catalytic Efficiency of Mesoporous Ti-MCM-41 Molecular Sieves. *Catal. Today*. **2008**, *133*, 639.
- (21) Eimer, G.; Chanquia, C.; Sapag, K.; Herrero, E. The Role of Different Parameters of Synthesis in the Final Structure of Ti-containing Mesoporous Materials. *Microporous Mesoporous Mater.* **2008**, *116* (1–3), 670.
- (22) Gregg, S.; Sing, K. *Adsorption Surface Area and Porosity*; Academic Press, Inc.: London, 1982.
- (23) Cagnoli, M.; Casuscelli, S.; Alvarez, A.; Bengoa, J.; Gallegos, N.; Samaniego, N.; Crivello, M.; Ghione, G.; Perez, C.; Herrero, E.; Marchetti, S. "Clean" Limonene Epoxidation using Ti-MCM-41 Catalyst. *Appl. Catal., A* **2005**, *287*, 227.
- (24) Eimer, G.; Pierella, L.; Anunziata, O.; Monti, G. Preparation and Characterization of Aluminium-Containing MCM-41. *Catal. Commun.* **2003**, *4*, 118.
- (25) Cedeño, L.; Hernandez, D.; Klimova, T.; Ramirez. Synthesis of Nb-Containing Mesoporous Molecular Sieves. Analysis of its Potential Use in HDS Catalyst. *Appl. Catal., A* **2003**, *241*, 39.
- (26) Bordiga, S.; Coluccia, S.; Lamberti, C.; Marchese, L.; Zecchina, A.; Boscherini, F.; Bufo, F.; Genoni, F.; Leofanti, G.; Petrini, G.; Vlaic, G. XAFS Study of Ti-Silicalite: Structure of Framework Ti(IV) in the Presence and Absence of Reactive Molecules ( $H_2O$ ,  $NH_3$ ) and Comparison with Ultraviolet-Visible and IR Results. *J. Phys. Chem. B* **1994**, *98*, 4125.
- (27) Ricchiardi, G.; Damin, A.; Bordiga, S.; Lamberti, C.; Spano, G.; Rivetti, F.; Zecchina, A. Vibrational Structure of Titanium Silicate Catalysts. A Spectroscopic and Theoretical Study. *J. Am. Chem. Soc.* **2001**, *121*, 11409.
- (28) Rajakovich, V.; Mintova, S.; Senker, J.; Bein, T. Synthesis and Characterization of V- and Ti-Substituted Mesoporous Materials. *Mater. Sci. Eng., C* **2003**, *23*, 817.
- (29) Choi, J.; Kim, D.; Chang, S.; Ahn, W. Catalytic Application of MCM-41 with Different Pore Size in Selected Liquid Phase Reactions. *Appl. Catal., A* **2003**, *254*, 225.
- (30) Trong On, D.; Nguyen, S.; Hulea, V.; Dumitriu, E.; Kaliaguine, S. Mono and Bifunctional MFI, BEA and MCM-41 Titanium-Molecular Sieves. Part I. Synthesis and Characterization. *Microporous Mesoporous Mater.* **2003**, *57*, 169.
- (31) Luo, Y.; Lu, G.; Guo, Y.; Wang, Y. Study on Ti-MCM-41 Zeolites Prepared with Inorganic Titanium Sources: Synthesis, Characterization and Catalysis. *Catal. Commun.* **2002**, *3*, 129.
- (32) Chao, M.; Lin, H.; Mou, C.; Cheng, B.; Cheng, C. Synthesis of Nano-Sized Mesoporous Silicas with Metal Incorporation. *Catal. Today* **2004**, *97*, 81.
- (33) Otero Areán, C.; Rodríguez Delgado, M.; Montouillout, V.; Lavallay, J.; Fernandez, C.; Cuatrecasas, J.; Parra, J. NMR and FTIR Spectroscopic Studies on the Acidity of Gallia-Silica Prepared by a Sol-Gel Route. *Microporous Mesoporous Mater.* **2004**, *67*, 259.
- (34) Conesa, T.; Hidalgo, J.; Luque, R.; Campelo, J.; Romero, A. Influence of the Acid-Base Properties in Si-MCM-41 and B-MCM-41 Mesoporous Materials on the Activity and Selectivity of  $\epsilon$ -Caprolactam Synthesis. *Appl. Catal., A* **2006**, *299*, 224.
- (35) Chen, L.; Norëna, L.; Navarrete, J.; Wang, J. Improvement of Surface Acidity and Structural Regularity Zr-Modified Mesoporous MCM-41. *Mater. Chem. Phys.* **2006**, *97* (2–3), 236.
- (36) Kruk, M.; Jaroniec, M. Characterization of High-Quality MCM-48 and SBA-1 Mesoporous Silicas. *Chem. Mater.* **1999**, *11* (9), 2568.
- (37) Kruk, M.; Jaroniec, M.; Sakamoto, Y.; Terasaki, O.; Ryoo, R.; Ko, C. Determination of Pore Size and Pore Wall Structure of MCM-41 by Using Nitrogen Adsorption, Transmission Electron Microscopy, and X-ray Diffraction. *J. Phys. Chem. B* **2000**, *104*, 292.
- (38) Díaz, I.; Pérez-Pariente, J. Synthesis of Spongelike Functionalized MCM-41 Materials from Gels Containing Amino Acids. *Chem. Mater.* **2002**, *14* (11), 4641.
- (39) Notari, B. Microporous Crystalline Titanium Silicates. *Adv. Catal.* **1996**, *41*, 253.
- (40) Lin, K.; Pescarmona, P.; Vandepitte, H.; Liang, D.; Van Tendeloo, G.; Jacobs, P. Synthesis and Catalytic Activity of Ti-MCM-41 Nanoparticles with Highly Active Titanium Sites. *J. Catal.* **2008**, *254*, 64.
- (41) Fraile, J.; García, J.; Mayoral, J.; Vispe, E. Optimization of Cyclohexene Epoxidation with Dilute Hydrogen Peroxide and Silica-Supported Titanium Catalyst. *Appl. Catal., A* **2003**, *245*, 363.
- (42) Chen, L.; Chuah, G.; Jaenicke, S. Ti-containing MCM-41 Catalyst for Liquid Phase Oxidation of Cyclohexene with Aqueous  $H_2O_2$  and Tert-butyl Hydroperoxide. *Catal. Lett.* **1998**, *50*, 107.
- (43) Peña, M.; Dellarocca, V.; Rey, F.; Corma, A.; Coluccia, S.; Marchese, L. Elucidating the Local Environment of Ti(IV) Active Sites in Ti-MCM-48: a Comparison between Silylated and Calcinated Catalyst. *Microporous Mesoporous Mater.* **2001**, *44/45*, 345.
- (44) Fraile, J.; García, J.; Mayoral, J.; Vispe, E. Silica-Supported Titanium Derivatives as Catalysts for the Epoxidation of Alkenes with Hydrogen Peroxide: A New Way to Tuneable Catalytic Activity through Ligand Exchange. *J. Catal.* **2000**, *189*, 40.

Received for review November 24, 2008

Revised manuscript received August 25, 2009

Accepted September 3, 2009

IE8018017